Phase-field approach to three-dimensional vesicle dynamics

Thierry Biben,[1] Klaus Kassner,[2] and Chaouqi Misbah[1,*]
[1]*LSP, Dynamique des Fluides Complexes et Morphogénèse, Université Joseph Fourier (CNRS), Grenoble I, B.P. 87, Saint-Martin d'Hères, 38402 Cedex, France*
[2]*Institut für Theoretische Physik, Otto-von-Guericke-Universität Magdeburg, Postfach 4120, D-39016 Magdeburg, Germany*
(Received 18 May 2005; published 20 October 2005)

We extend our recent phase-field [T. Biben and C. Misbah, Phys. Rev. E **67**, 031908 (2003)] approach to 3D vesicle dynamics. Unlike the boundary-integral formulations, based on the use of the Oseen tensor in the small Reynolds number limit, this method offers several important flexibilities. First, there is no need to track the membrane position; rather this is automatically encoded in dynamics of the phase field to which we assign a finite width representing the membrane extent. Secondly, this method allows naturally for any topology change, like vesicle budding, for example. Thirdly, any non-Newtonian constitutive law, that is generically nonlinear, can be naturally accounted for, a fact which is precluded by the boundary integral formulation. The phase-field approach raises, however, a complication due to the local membrane incompressibility, which, unlike usual interfacial problems, imposes a nontrivial constraint on the membrane. This problem is solved by introducing dynamics of a tension field. The first purpose of this paper is to show how to write adequately the advected-field model for 3D vesicles. We shall then perform a singular expansion of the phase field equation to show that they reduce, in the limit of a vanishing membrane extent, to the sharp boundary equations. Then, we present some results obtained by the phase-field model. We consider two examples; (i) kinetics towards equilibrium shapes and (ii) tanktreading and tumbling. We find a very good agreement between the two methods. We also discuss briefly how effects, such as the membrane shear elasticity and stretching elasticity, and the relative sliding of monolayers, can be accounted for in the phase-field approach.

DOI: 10.1103/PhysRevE.72.041921 PACS number(s): 87.10.+e, 87.16.Ac, 87.16.Dg, 87.19.St

I. INTRODUCTION

Problems in which moving interfaces are involved, like fluid-fluid, solid-fluid interfaces, and membranes, have been traditionally treated by considering the boundary as a geometrical location (a mathematical surface having no width), and on which one has to impose boundary conditions in connection with the underlying fields describing dynamics (for example heat flow in crystal growth, hydrodynamic flow for fluid interfaces, and so on). This is completely justified inasmuch as the real interfacial region is usually of atomic thickness, while the size and the patterns of interest are much larger. Many problems have been successfully solved by this method, in crystal growth [1,2], for fluid interfaces in the small Reynolds number limit [3], for capsules mimicking red blood cells [4], for biological vesicles [5,6], and so on. These methods used either boundary integral formulations based on the Green's [1,2] function [3] (this is possible when the bulk equations are linear), or by discretizing the bulk equations in both phases and match them at the interface via the imposed boundary equations [7]. The latter method is not limited to linear equations in the bulk phase. One of the drawbacks of the latter method, however, is that one has to follow explicitly the interface position, and refine the grid in the vicinity of the interface in situations where the dynamics, for example, involve singularities, or boundary layers. A typical situation is the Grinfeld instability which is known to lead to a finite time cusp singularity [7,8]. The finite elements method used for the Grinfeld instability [7], albeit quite efficient, is not always easy to implement, and may not be capable of resolving some singularities [7]. In addition this kind of (boundary-tracking) method does not allow automatically to treat a topology change, such as breakup of a vesicle into smaller ones, unless some specific prescription is fixed (and often this is done in an *ad hoc* manner). Boundary integral formulations also have their shortcomings. First, they do not allow for a topology change, and secondly, and this is a more serious limitation, they are limited to situations where the bulk equations are linear. In addition, this method is not always flexible (for example adding a viscosity contrast requires some deal, whereas with a phase field approach this is rather straightforward, as we shall comment later).

More recently, several communities have adopted another type of method, known in the physicist community as the phase field model. The crux of this model is the introduction of an auxiliary field, ϕ, which is a function of space and time. The dynamics of this field is written in such a way that it takes a value, say, $\phi=-1$ in one of the two bulk phases, and $\phi=1$ in the other phase. This field varies abruptly in a $\tanh(r/\epsilon)$ manner, where ϵ is a small parameter measuring the width of the boundary (e.g., interface, membrane), and r is a coordinate along the interface normal. Thus there is no explicit prescription of the boundary. Rather, this is encoded in the rapid variation of ϕ. This field is, in some sense, passive and is coupled to the relevant dynamical variables (like the velocity field) of the problem under consideration. This type of modeling has become popular in solving interfacial problems, and has been developed in various contexts like solidification [9], elastic instabilities [10,11], fracture

*Email address: chaouqi.misbah@ujf-grenoble.fr

[12], droplet-breakup [13], fluid-fluid interfaces in a Hele-Shaw problem [15], etc. The success of the method is at least fourfold. (i) It is relatively easy to implement (in comparison to finite elements or boundary integral formulations), (ii) it does not require a front tracking, (iii) it allows naturally for a topology change, and (iv) it can be adopted to diverse situations, including the one where the underlying equations are nonlinear. Other methods, which are similar in spirit, have been developed, more often in the computer scientist and applied mathematics communities. These are, among other methods, the level set and volume of fluid methods [16,17].

In a recent work we have presented a brief account on the use of the phase-field method to vesicle dynamics [13], and more recently an attempt has been made along this direction without hydrodynamic flow [14]. In our previous work [13], most of our focus was directed towards the use of the method in the context of tumbling. This paper is devoted to an extensive discussion to the method itself. We generalize here the method to 3D, and perform the sharp boundary limit in order to show that asymptotically the model recovers the usual equations. We shall also discuss how other effects, like monolayers sliding and permeability across the membrane, can be incorporated in the model. We show numerical results of relaxation towards equilibrium shapes, and the behavior of vesicles in an external shear flow.

The scheme of this paper is as follows. In Sec. II we introduce the model. The sharp boundary limit is performed in Sec. III. Section IV is devoted to the study of some dynamical examples, and a summary and discussion constitute the topic of Sec. V. Many technical details are relegated into three Appendixes.

II. THE PHASE-FIELD MODEL

In this section we write down the phase field (PF) model for vesicles in 3D by following a similar spirit as that in 2D [13]. Let ϕ designate the PF which takes the value $\phi=-1$ in the interior and $\phi=1$ in the exterior, respectively. The field is advected by the flow, and is forced to take these two values inside and outside the vesicle thanks to a double well potential. Thus its dynamics is given by

$$\frac{\partial \phi}{\partial t} = -\mathbf{v}\cdot\nabla\phi + \Gamma\left(\nabla^2\phi - \frac{1}{4\epsilon^2}g'(\phi) + \hat{c}|\nabla\phi|\right), \qquad (1)$$

where we have Γ as a parameter (its magnitude with respect to ϵ will be specified later). The first term on the right-hand side (RHS) of the equation is the advection one ($\mathbf{v}$ is the fluid velocity), the second is a wall-like energy, the third one is the double well where $g(\phi)=(1-\phi^2)^2$ and the last term is introduced [15] in order to cancel the leading order contribution coming from the wall term; the wall term introduces a surface-like energy which is not desirable especially for vesicles which are devoid of a surface energy. The formal cancellation will be shown in the next section. We have introduced the curvature

$$\hat{c} = -\nabla\cdot\hat{\mathbf{n}}, \qquad (2)$$

where $\hat{\mathbf{n}}=\nabla\phi/|\nabla\phi|$ is the normal vector to the contour surfaces of the PF. That is, $\hat{c}$ is the mean curvature, defined as the sum of the two principal curvatures of the contour surface at the position of the normal. In the next section it will become clear how the orders of magnitude in terms of the small parameter are chosen.

Since vesicle motion is accompanied with a hydrodynamic flow, we need to describe the velocity field. While the method can be developed for arbitrary Reynolds number, we shall specialize it to the small Reynolds number limit since we have in mind only application to vesicles in this paper. The velocity field equations are written as

$$\epsilon_v\frac{\partial \mathbf{v}}{\partial t} = \nabla\cdot\sigma - \nabla p + \mathbf{F}_c + \mathbf{F}_\xi, \qquad (3)$$

$$\nabla\cdot\mathbf{v} = 0. \qquad (4)$$

The first one is the momentum transport equation, while the second one is the incompressibility condition. The LHS of Eq. (3) represents an inertial-like term. Since we shall choose ϵ_v to be small enough, this amounts practically to taking the pure Stokes limit (the pure viscous limit). The stress tensor is $\sigma=\eta(\phi)\{\nabla\mathbf{v}+(\nabla\mathbf{v})^T\}$, where $\eta(\phi)$ accounts for a possible viscosity contrast between the interior and the exterior of the vesicle; a convenient prescription is $\eta(\phi)=(1+\phi)\eta_{out}/2+(1-\phi)\eta_{in}/2$, where η_{out} and η_{in} are the bulk viscosities outside and inside the vesicle, respectively. While our numerical results have been performed for arbitrary viscosity contrasts, in the derivation of the sharp boundary limit we shall restrict ourselves to the free contrast case where η is simply a constant. The extension of our derivation to the general case presents no specific complication.

The forces appearing on the RHS are the curvature force, $\mathbf{F}_c$, associated with the bending rigidity, and the tension-like force, $\mathbf{F}_\xi$, associated with the fact that the local area of the membrane is preserved under dynamics (there is neither stretching nor compression under dynamics). This force is associated with a Lagrange multiplier ξ which is a function of time and of the position on the membrane. More precisely, the energy associated with membrane bending and incompressibility is written as

$$H = \frac{\kappa}{2}\int d\mathbf{r}(\hat{c}-c_0)^2\frac{|\nabla\phi|}{2} + T\int d\mathbf{r}\ \xi(\mathbf{r},t)\frac{|\nabla\phi|}{2}. \qquad (5)$$

κ is the membrane rigidity, c_0 is a spontaneous curvature, and T is a tensionlike parameter (making ξ dimensionless) and the factor $|\nabla\phi|/2$ is there in order that the action of the rigidity and the tension be localized on the membrane; it plays the role of a surface Dirac function and this will become more visible below. The idea of the PF is precisely not to make it a pure Dirac function but to leave it in principle extended (or diffuse), albeit localized enough in order to have, as close as possible, the required degree of precision. The forces are obtained from the functional derivative of the energy upon a virtual displacement of the membrane position. We have thus (the details of the derivation are given in Appendix A)

$$\mathbf{F}_c \equiv -\frac{\delta H_c}{\delta \mathbf{R}} = -\frac{\kappa}{2}\boldsymbol{\nabla}\cdot\left\{\frac{(1-\hat{\mathbf{n}}\hat{\mathbf{n}})}{|\boldsymbol{\nabla}\phi|}\cdot\boldsymbol{\nabla}[(\hat{c}-c_0)|\boldsymbol{\nabla}\phi|]+\frac{(\hat{c}-c_0)^2}{2}\hat{\mathbf{n}}\right\}\times|\boldsymbol{\nabla}\phi|\hat{\mathbf{n}}. \quad (6)$$

The tensionlike force takes the form (see Appendix A)

$$\mathbf{F}_\xi = T\left[\xi\hat{c}\frac{\boldsymbol{\nabla}\phi}{2}+(1-\hat{\mathbf{n}}\hat{\mathbf{n}})\cdot\boldsymbol{\nabla}\xi\frac{|\boldsymbol{\nabla}\phi|}{2}\right]. \quad (7)$$

It will be shown below from the sharp boundary limit that to leading order, the curvature force can be written as

$$\mathbf{F}_c = -\kappa\left[\frac{1}{2}(\hat{c}-c_0)[\hat{c}(\hat{c}+c_0)-4\hat{G}]+\Delta_{2D}\hat{c}\right]\frac{\boldsymbol{\nabla}\phi}{2}, \quad (8)$$

where

$$\hat{G} = \det[(\hat{\mathbf{t}}_1\cdot\boldsymbol{\nabla})\hat{\mathbf{n}},(\hat{\mathbf{t}}_2\cdot\boldsymbol{\nabla})\hat{\mathbf{n}},\hat{\mathbf{n}}] \quad (9)$$

is the Gaussian curvature of the contour surface, and by $\hat{\mathbf{n}}\hat{\mathbf{n}}$ we denote the projection operator projecting on the normal vector $\hat{\mathbf{n}}$. Hence, $1-\hat{\mathbf{n}}\hat{\mathbf{n}}$ projects onto the tangential plane. The dot in (7) signifies a multiplication between a matrix and a vector. Subscripts 2D characterize differential operators on contour surfaces. Specifically, Δ_{2D} is the Laplace-Beltrami operator, given by

$$\Delta_{2D} = [(1-\hat{\mathbf{n}}\hat{\mathbf{n}})\cdot\boldsymbol{\nabla}]\cdot[(1-\hat{\mathbf{n}}\hat{\mathbf{n}})\cdot\boldsymbol{\nabla}], \quad (10)$$

and $\boldsymbol{\nabla}_{2D}\cdot\mathbf{v}$ is the surface divergence of $\mathbf{v}$:

$$\boldsymbol{\nabla}_{2D}\cdot\mathbf{v} = [(1-\hat{\mathbf{n}}\hat{\mathbf{n}})\cdot\boldsymbol{\nabla}]\cdot\mathbf{v}. \quad (11)$$

Expression (8) is nothing but the well known Helfrich force [20] in 3D.

One of the new questions that arises when treating vesicles, in comparison to front problems for which a myriad of phase field models have been developed, is the incompressibility condition of the membrane. This sets a serious constraint on the dynamics. As time elapses the hydrodynamics flow field changes and so does the set of forces acting on the membrane. In other words, the initial value of the Lagrange multiplier ξ is not necessarily the one that is required to preserve area later on. Thus we have in principle to determine ξ at each time. One possible way would be to evaluate at each time the change of the local area, then require that the area be the same as the original one, and evaluate the tension fields that satisfies this constraint. Instead of making these various steps, we introduce an evolution equation of the tension field that is valid everywhere in the bulk (by doing so we do not need to track the boundary). The suggested type of equation is an equation that forces the local area on a short enough time scale and to relax back to the originally prescribed one. Since a change of the local area is dictated by the surface divergence of the velocity field, the evolution equation has the form

$$\frac{\partial\xi}{\partial t} = D_\xi\boldsymbol{\nabla}^2\xi-\mathbf{v}\cdot\boldsymbol{\nabla}\xi+\boldsymbol{\nabla}_{2D}\cdot\mathbf{v}. \quad (12)$$

The term $-\mathbf{v}\cdot\boldsymbol{\nabla}\xi$ is simply the advection term telling that the tension field must follow the membrane according to the actual fluid velocity adjacent to the membrane. The diffusion term is introduced for regularization purpose in the numerical scheme. From the formal point of view it will be shown that its introduction renders the statement about the sharp boundary limit nonambiguous, as we shall see below. If the diffusion term were absent we would have a direct proportionality between the material derivative of ξ and the surface divergence. We shall require ξ to be of order ϵ (and T to be of order $1/\epsilon$ so that the product remains of order unity) and thus to leading order we expect the evolution equation of ξ to be dominated by $\boldsymbol{\nabla}_{2D}\cdot\mathbf{v}\simeq 0$, thus the required condition. This is what will be shown formally below.

Before exploiting the model extensively it will first be essential to show that the above set of equations reduce to the sharp boundary equations in the limit when $\epsilon\to 0$. This step was not yet described in our previous work in 2D [13]. Here we shall show it directly in 3D, and obviously the 2D limit is straightforward from the 3D results.

III. THE SHARP BOUNDARY LIMIT

The sharp boundary (SB) limit is a singular one in the sense that we cannot just take the limit $\epsilon=0$ in the set of equations (1), (3), (4), and (12). As is seen on Eq. (1), for example, upon multiplication of both sides by ϵ^2, ϵ multiplies the highest derivative (the $\boldsymbol{\nabla}^2$) and thus it is a singular perturbation, leading to a boundary layer; that is a region of extent ϵ inside which the field ϕ varies abruptly. In this type of problems one has to distinguish between two regions: the *inner* region, which is confined to a distance of order ϵ about the boundary where ϕ has a rapid variation, and an *outer* region, which is the complementary region, away from the boundary, where ϕ varies smoothly. Standard matching conditions are obtained from the requirement that the asymptotic expansions of the inner domain and the outer domain agree in a region of overlap.

In order to deal with the inner region, which is a bit more tricky, we first introduce local coordinates in the vicinity of the membrane. Besides the normal vector, we need two linearly independent tangent vectors to contour surfaces, which we denote by $\hat{\mathbf{t}}_1$ and $\hat{\mathbf{t}}_2$. We choose these three vectors to form an orthonormal trihedron, i.e., we take them as unit vectors and set $\hat{\mathbf{t}}_2=\hat{\mathbf{n}}\times\hat{\mathbf{t}}_1$. They are not identical to the normal and tangents at the SB which shall be simply denoted by $\mathbf{n}$, $\mathbf{t}_1$, and $\mathbf{t}_2$. However, $\hat{\mathbf{t}}_1$, $\hat{\mathbf{t}}_2$, and $\hat{\mathbf{n}}$ will approach $\mathbf{t}_1$, $\mathbf{t}_2$ and $\mathbf{n}$, respectively, in the limit $\epsilon\to 0$ on contours approaching the interface. Outside the interface, the limit is indefinite. We then set $\mathbf{r}=\mathbf{R}(s,u)+r\mathbf{n}(s,u)$, where $\mathbf{R}$ is the membrane position and s, u are orthogonal coordinates on the membrane, parametrized such that they indicate arclengths along the coordinate curves $(r,u)=$const and $(r,s)=$const, respectively. This means that $|\partial\mathbf{R}/\partial s|=|\partial\mathbf{R}/\partial u|=1$ and $\mathbf{t}_1=\partial\mathbf{R}/\partial s$, $\mathbf{t}_2=\partial\mathbf{R}/\partial u$. $\mathbf{t}_1$, $\mathbf{t}_2$, and $\mathbf{n}$ form a right-handed trihedron. In order to simplify the following derivations, we choose the coordi-

nate lines to be geodesics. A general relationship between the geodesic curvature α of a curve on a surface (i.e., its in-surface curvature), its normal curvature γ, and its curvature κ_s as a space curve is

$$\kappa_s^2 = \alpha^2 + \gamma^2. \tag{13}$$

Geodesics are the analogs of straight lines on the surface, so their geodesic curvature is zero by definition, which means that the normal curvature of our coordinate lines coincides with their spatial curvature. This results in simplified equations of motion for the Bonnet-Kowalewski trihedron [19] moving along such a curve. They become identical to the Frenet formulas:

$$\frac{\partial \mathbf{n}}{\partial s} = -c_1 \mathbf{t}_1 - \tau_1 \mathbf{t}_2,$$

$$\frac{\partial \mathbf{t}_1}{\partial s} = c_1 \mathbf{n}, \quad \frac{\partial \mathbf{t}_2}{\partial s} = \tau_1 \mathbf{n},$$

$$\frac{\partial \mathbf{n}}{\partial u} = -c_2 \mathbf{t}_2 + \tau_2 \mathbf{t}_1,$$

$$\frac{\partial \mathbf{t}_1}{\partial u} = -\tau_2 \mathbf{n}, \quad \frac{\partial \mathbf{t}_2}{\partial u} = c_2 \mathbf{n}, \tag{14}$$

where c_1 and c_2 are the curvatures of the space curves described by the coordinate lines corresponding to s and u, respectively, whereas τ_1 and τ_2 are their torsions. Note that the usual right-handed Frenet trihedron is given by $\mathbf{t}_1$, $\mathbf{n}$, $-\mathbf{t}_2$ for coordinate s and by $\mathbf{t}_2$, $\mathbf{n}$, $\mathbf{t}_1$ for u.

To obtain the metric tensor associated with these coordinates, we first calculate the induced base vectors:

$$\mathcal{E}_r \equiv \frac{\partial \mathbf{r}}{\partial r} = \mathbf{n}(s,u),$$

$$\mathcal{E}_s \equiv \frac{\partial \mathbf{r}}{\partial s} = \frac{\partial \mathbf{R}}{\partial s} + r\frac{\partial \mathbf{n}}{\partial s} = (1 - rc_1)\mathbf{t}_1 - r\tau_1 \mathbf{t}_2,$$

$$\mathcal{E}_u \equiv \frac{\partial \mathbf{r}}{\partial u} = \frac{\partial \mathbf{R}}{\partial s} + r\frac{\partial \mathbf{n}}{\partial u} = (1 - rc_2)\mathbf{t}_2 + r\tau_2 \mathbf{t}_1. \tag{15}$$

Note that this canonical basis is orthogonal on the membrane (i.e., for $r=0$) but becomes nonorthogonal off it, due to the presence of the torsion terms. This complication does not arise in a two-dimensional system with a one-dimensional interface, because there the derivative of $\mathbf{n}$ is always parallel to that of $\mathbf{R}$, whereas here it can have a component in the direction of $\mathbf{t}_2$ for s and one in the direction of $\mathbf{t}_1$ for u.

The components of the metric tensor are given by $g_{ij} = \mathcal{E}_i \mathcal{E}_j$, where $i,j \in \{r,s,u\}$. Before writing them out, we exploit a symmetry to exhibit some interdependencies between the normal curvatures and the torsions. Due to the interchangeability of partial derivatives, we have

$$\partial_j \mathcal{E}_i = \partial_j \partial_i \mathbf{r} = \partial_i \mathcal{E}_j, \tag{16}$$

which is automatically satisfied for the mixed derivatives containing r as a variable. But equating $\partial_u \mathcal{E}_s = \partial_s \mathcal{E}_u$, we obtain

$$\tau_1 = -\tau_2 \equiv \tau,$$

$$c_{1u} = -\tau_{2s} = \tau_s, \quad c_{2s} = \tau_{1u} = \tau_u, \tag{17}$$

where subscripts s and u denote partial derivatives with respect to these variables. The metric g_{ij} can then be obtained directly along with the contravariant g^{ij} version of the metric tensor and its determinant g, as listed in Eqs. (B1)–(B3) in Appendix B. The vectors of the reciprocal basis are given by $\mathcal{E}^i = g^{ij}\mathcal{E}_j$ [see expression (B4) in Appendix B]; we use the Einstein summation convention throughout. We are now in a position to express differential operators in terms of the inner coordinates, as shown in Appendix B. As an example let us write the gradient:

$$\begin{aligned}\boldsymbol{\nabla} &= \mathcal{E}^i \partial_i \\ &= \mathbf{n}\partial_r + \frac{1}{(1 - rc_1)(1 - rc_2) - r^2\tau^2}\{\mathbf{t}_1[(1 - rc_2)\partial_s + r\tau\partial_u] \\ &\quad + \mathbf{t}_2[r\tau\partial_s + (1 - rc_1)\partial_u]\}.\end{aligned} \tag{18}$$

The divergence and Laplacian are listed in Appendix B.

The next step is to perform a stretching transformation via introduction of a fast coordinate $\rho = r/\epsilon$. The resulting expressions for differential operators are trivially obtained from Eqs. (18)–(58), (A1)–(A15), and (B1)–(B7): each derivative with respect to r acquires a factor $1/\epsilon$ when replaced by a derivative with respect to ρ. Finally, each field in the outer and inner regions is expanded in powers of ϵ. In order to distinguish the inner fields from the outer ones, we denote them by capital letters. For example, the field ϕ in the outer and inner regions is written as

$$\phi(x,y,z,t) = \phi_0(x,y,z,t) + \epsilon\phi_1(x,y,z,t) + \cdots,$$

$$\Phi(\rho,s,u,t) = \Phi_0(\rho,s,u,t) + \epsilon\Phi_1(\rho,s,u,t) \tag{19}$$

and similar conventions are used for the other fields (velocity and tension in the inner and outer regions are written as $\mathbf{v}$, $\mathbf{V}$ and ξ and X). We then require the inner solution to match the outer one in a domain of overlap.

Finally note that since the interface will move in general and the coordinates ρ, s, u are defined with respect to the interface, there is also a transformation rule for the time derivative:

$$\partial_t f(x,y,z,t) = \partial_t F(\rho,s,u,t) - \mathbf{W} \cdot \boldsymbol{\nabla} F(\rho,s,u,t), \tag{20}$$

where $\mathbf{W}(s,u,t) = \mathbf{w}[x(s,u),y(s,u),z(s,u),t]$ is the interface velocity. Equation (20) exhibits that the time derivative in the comoving frame is a material derivative. In order to formulate the matching conditions concisely, we will occasionally also write the outer fields as functions of the variables r, s, and u (without changing their naming letter, thus in this case adhering to the physicists' convention of using a letter for a physical quantity instead of a mathematical function). Moreover, when describing the limit of an outer field, say the pressure p, as the interface is approached from the side of positive or negative r, respectively, we will just use a superscript $+$ or $-$, i.e., $p^{\pm} = p^{\pm}(s,u,t) = \lim_{r \to \pm 0} p(r,s,u,t)$. In order to complete our preliminaries, we need for the inner equations an expression for the modulus of the gradient of ϕ

(up to some useful order in ϵ). Using the approximation (B10) for the gradient we find

$$|\nabla\Phi| = \frac{1}{\epsilon}|\partial_\rho\Phi|E_{\epsilon\Phi}, \tag{21}$$

where

$$E_{\epsilon\Phi} \equiv \left[1 + \left(\frac{\epsilon}{1-\epsilon\rho c_1}\frac{\partial_s\Phi}{\partial_\rho\Phi} + \epsilon^2\rho\tau\frac{\partial_u\Phi}{\partial_\rho\Phi}\right)^2 + \left(\frac{\epsilon}{1-\epsilon\rho c_2}\frac{\partial_u\Phi}{\partial_\rho\Phi} + \epsilon^2\rho\tau\frac{\partial_s\Phi}{\partial_\rho\Phi}\right)^2\right]^{1/2} + O(\epsilon^3),$$

$$= 1 + O(\epsilon^2) \tag{22}$$

and we have chosen r to increase from the side of the interface where Φ is negative (the inside) to the one where Φ is positive (the outside). As a consequence, $\partial_\rho\Phi$ is positive.

The strategy now is to use the set of complete equations (1), (3), (4), and (12), expand them according to (19), together with the differentiation operators in the inner region given in Appendix B, and deduce successively higher orders in powers of ϵ.

Leading order expansion

1. Outer solution

In the outer region we use the original spatial variables (not the stretched one). Collect the dominant terms in ϵ (which are $\sim\epsilon^{-2}$) from Eq. (1) we obtain

$$\frac{1}{4}g'(\phi_0) = -\phi_0(1-\phi_0^2) = 0, \tag{23}$$

with the solutions

$$\phi_0 = 0, \pm 1. \tag{24}$$

The solution $\phi_0=0$ sits on a maximum of the free-energy functional leading to Eq. (1) and is unstable, whereas the two other solutions, which are stable, correspond to the desired limits of the PF at the inside and outside of the vesicle, respectively. It should be noted that $\phi_0=\pm 1$ remains a solution of Eq. (1) at arbitrary order in ϵ. Thus (8) and (7) vanish implying that (3) and (4) reduce to the Stokes equations. Equation (12) becomes, since $\xi=O(\epsilon)$, $\nabla_{2D}\mathbf{v}=0$, i.e., it enforces the area constraint of the membrane. Apart from that, the outer equations provide, via the matching conditions, boundary conditions for the solutions of the inner ones, as will be seen below.

2. Inner solution

The inner equation for Φ becomes at leading order

$$\partial_\rho^2\Phi_0 - \frac{1}{4}g'(\phi_0) = \partial_\rho^2\Phi_0 + \Phi_0(1-\Phi_0^2) = 0, \tag{25}$$

which together with the matching conditions

$$\lim_{\rho\to\pm\infty}\Phi_0(\rho) = \phi_0^\pm = \pm 1, \tag{26}$$

leads to the unique solution

$$\Phi_0 = \Phi_0(\rho) = \tanh(\rho/\sqrt{2}). \tag{27}$$

The important fact to note is that Φ_0 does not depend on s nor u, which enables tremendous simplifications. For example, it should be immediately clear that instead of the last equation in (22), we even have

$$E_{\epsilon\Phi} = 1 + O(\epsilon^3), \tag{28}$$

because the derivatives of Φ with respect to s and u are $O(\epsilon)$ already.

In what follows we will also need expressions for the normal and tangential vectors to the contour surfaces. From $\hat{\mathbf{n}}=\nabla\Phi/|\nabla\Phi|$, we have

$$\hat{\mathbf{n}} = \frac{1}{E_{\epsilon\Phi}}\left(\mathbf{n} + \frac{\epsilon}{1-\epsilon\rho c_1}\frac{\partial_s\Phi}{\partial_\rho\Phi}\mathbf{t}_1 + \frac{\epsilon}{1-\epsilon\rho c_2}\frac{\partial_u\Phi}{\partial_\rho\Phi}\mathbf{t}_2\right) + O(\epsilon^3)$$
$$= \mathbf{n} + O(\epsilon^2). \tag{29}$$

The tangential vectors are to be defined such that their limits for $\epsilon\to 0$ become $\mathbf{t}_1$ and $\mathbf{t}_2$, respectively. This is achieved by setting

$$\hat{\mathbf{t}}_1 = E_{\epsilon\Phi}\left(\mathbf{t}_1 - \frac{\epsilon}{1-\epsilon\rho c_1}\frac{\partial_s\Phi}{\partial_\rho\Phi}\mathbf{n}\right) + O(\epsilon^3) = \mathbf{t}_1 + O(\epsilon^2), \tag{30}$$

$$\hat{\mathbf{t}}_2 = \hat{\mathbf{n}}\times\hat{\mathbf{t}}_1 = \mathbf{t}_2 - \frac{\epsilon}{1-\epsilon\rho c_2}\frac{\partial_u\Phi}{\partial_\rho\Phi}\mathbf{n} + O(\epsilon^3) = \mathbf{t}_2 + O(\epsilon^2). \tag{31}$$

The higher-order terms in (30) can be arranged such that $\hat{\mathbf{t}}_1$ is a unit vector, which implies that $\hat{\mathbf{t}}_2$ is one, too. It is then straightforward to calculate the Gaussian curvature of a contour surface according to Eq. (9), with the result

$$\hat{G} = \frac{c_1c_2-\tau^2}{(1-\epsilon\rho c_1)(1-\epsilon\rho c_2)} + O(\epsilon^2) = \frac{G}{1-\epsilon\rho c} + O(\epsilon^2). \tag{32}$$

In addition, to get the explicit form of the inner equations, we need

$$\nabla_{2D} = \mathbf{t}_1\partial_s + \mathbf{t}_2\partial_u + O(\epsilon), \tag{33}$$

$$\Delta_{2D} = \partial_s^2 + \partial_u^2 + O(\epsilon), \tag{34}$$

$$\hat{c} = c + \epsilon\rho c^2 - 2\epsilon\rho G + O(\epsilon^2). \tag{35}$$

After writing the dynamical equations in the inner variable, and using the results listed in Appendix B, we find that to leading order, Eqs. (B14)–(B16) yield

$$\partial_\rho^2\mathbf{V}_0 = 0, \tag{36}$$

from which we conclude that

$$\mathbf{V}_0 = \mathbf{V}_0(s) + \rho\mathbf{B}(s). \tag{37}$$

The matching condition that the velocity must remain finite in the outer region near the interface then tells us that $\mathbf{B}(s)\equiv 0$. Hence,

$$V_{0n} = V_{0n}(s,u,t), \tag{38}$$

$$V_{0t1} = V_{0t1}(s,u,t), \tag{39}$$

$$V_{0t2} = V_{0t2}(s,u,t). \tag{40}$$

In view of this result, the leading order of the divergence equation (B17) does not give anything new, we just obtain $\partial_\rho V_{0n}=0$.

Finally, from Eq. (B18), we have, at order ϵ^{-1}

$$\partial_\rho^2 X_1 = 0, \tag{41}$$

from which we conclude

$$X_1 = X_1(s,u,t). \tag{42}$$

We now have exploited all the inner equations to leading order.

Proceeding to the first subdominant order of the inner equations, we get from Eq. (B13) at order ϵ^{-1}

$$(V_{0n} - W_n)\partial_\rho \Phi_0 = \Gamma\left(\partial_\rho^2 \Phi_1 - \frac{1}{4} g''(\Phi_0)\Phi_1\right), \tag{43}$$

which may be rewritten as

$$\mathcal{L}\Phi_1 = \frac{1}{\Gamma}(V_{0n} - W_n)\partial_\rho \Phi_0, \tag{44}$$

where the linear operator $\mathcal{L}=\partial_\rho^2 - g''(\Phi_0)/4$ is Hermitian. The Fredholm alternative tells us that for this (possibly) inhomogeneous equation to be solvable the right-hand side must be orthogonal to all left null eigenvectors of $\mathcal{L}$. Since $\mathcal{L}$ is Hermitian, left and right eigenvectors are the same. But we know already a right null eigenvector of $\mathcal{L}$, as a consequence of translational invariance:

$$\mathcal{L}\partial_\rho \Phi_0 = \partial_\rho^2 \partial_\rho \Phi_0 - \frac{1}{4} g''(\Phi_0)\partial_\rho \Phi_0 = \partial_\rho\left(\partial_\rho^2 \Phi_0 - \frac{1}{4} g'(\Phi_0)\right) = 0, \tag{45}$$

where the last equality follows from Eq. (25), i.e., the fact that Φ_0 is a solution of the leading-order inner problem. Therefore, we must have

$$0 = \int_{-\infty}^{\infty} d\rho \frac{1}{\Gamma}[V_{0n}(s,u) - W_n(s,u)](\partial_\rho \Phi_0)^2$$

$$= \frac{1}{\Gamma}[V_{0n}(s,u) - W_n(s,u)] \int_{-\infty}^{\infty} d\rho (\partial_\rho \Phi_0)^2, \tag{46}$$

which implies, due to the positivity of the integrand

$$V_{0n}(s,u,t) = W_n(s,u,t), \tag{47}$$

the equality of the normal velocity of the liquid with that of the interface. It also shows that Eq. (44) is in fact a homogeneous equation.

Using Eqs. (27) and (38)–(40), we obtain at order ϵ^{-1} from Eq. (B14)

$$0 = \eta\partial_\rho^2 \mathbf{V}_1 - \mathbf{n}\partial_\rho P_0 + \left(\left\{-\kappa\left[\frac{1}{2}c(c^2-4G) + (\partial_s^2 + \partial_u^2)c\right] + c\tilde{T}X_1\right\}\mathbf{n} + \tilde{T}(\mathbf{t}_1\partial_s X_1 + \mathbf{t}_2\partial_u X_1)\right)\frac{1}{2}\partial_\rho \Phi_0. \tag{48}$$

Multiplying this by $\mathbf{n}$, we get

$$\eta\partial_\rho^2 V_{1n} = \partial_\rho P_0 + \frac{1}{2}\partial_\rho \Phi_0\left\{\kappa\left[\frac{1}{2}c(c^2-4G) + c_{ss} + c_{uu}\right] - c\tilde{T}X_1\right\}, \tag{49}$$

where we have used the fact that the base vector $\mathbf{n}$ is independent of ρ. Moreover, from the divergence equation we obtain at order ϵ^0

$$\partial_\rho V_{1n} = cV_{0n} - \partial_s V_{0t1} - \partial_u V_{0t2}. \tag{50}$$

Since all the components of $\mathbf{V}_0$ are independent of ρ [see Eqs. (38)–(40)], differentiation of (50) with respect to ρ yields $\partial_\rho^2 V_{1n}=0$, and Eq. (49) then provides a relationship for $\partial_\rho P_0$ that can be easily integrated. Taking the limits of integration to be $-\infty$ and ∞ we find with the help of the matching conditions $\lim_{\rho\to\pm\infty} P_0(\rho)=p_0^\pm$ and $\lim_{\rho\to\pm\infty} X_1(\rho,s,u,t) = X_1(s,u,t)=\xi_1(s,u,t)$

$$p_0^+(s,u,t) - p_0^-(s,u,t) = -\kappa\left[\frac{1}{2}(c-c_0)[(c+c_0)c - 4G] + c_{ss} + c_{uu}\right] + c\tilde{T}\xi_1, \tag{51}$$

which is the condition for local mechanical equilibrium at the interface. The velocity terms in Eq. (3) do not generate an interface force, because the velocity stress tensor (whose divergence is $\eta\boldsymbol{\nabla}^2\mathbf{v}$) is continuous across the interface. So all of the pressure difference has to come from $\mathbf{F}_c$. We recognize the Helfrich force as given in Eq. (8) and the normal part (the first term) of the tensionlike force [Eq. (7)] written in local coordinates.

Now projecting Eq. (48) on one of the two tangent vectors (say $\mathbf{t}_1$), we obtain

$$\eta\partial_\rho^2 V_{1t_1} = \tilde{T}\partial_s X_1 \frac{1}{2}\partial_\rho \Phi_0. \tag{52}$$

Integrating over ρ from $-\infty$ to $+\infty$ and due to the matching condition $\partial_\rho V_{1t_1}|_{\rho=\pm\infty} = \partial v_{0t_1}|_{r=0^\pm}$, we finally obtain

$$\eta\partial_\rho v_{0t_1} = \tilde{T}\partial_s X_1 \tag{53}$$

which is the balance of the tangential viscous force. A similar expression is obtained for the tangential component along $\mathbf{t}_2$.

Finally consider the first subdominant order of Eq. (12). It reads [exploiting Eq. (42)]

$$0 = D_\xi \partial_\rho^2 X_2 - cV_{0n} + \partial_s V_{0t1} + \partial_u V_{0t2}. \tag{54}$$

Now the matching conditions for X_2 are

$$X_2 \sim \xi_2(\pm 0,s,u,t) + \rho\partial_n\xi_1\,(r,s,ut)|_{r=\pm 0} \quad (\rho \to \pm\infty) \tag{55}$$

since $\xi_0=0$. On the other hand, integrating Eq. (54), we obtain, taking advantage of the fact that $\mathbf{V}_0$ does not depend on ρ:

$$X_2(\rho) = a(s,u) + b(s,u)\rho - \frac{\rho^2}{2D_\xi}(-cV_{0n} + \partial_s V_{0t1} + \partial_u V_{0t2}). \tag{56}$$

The only way for Eqs. (55) and (56) to be compatible with each other is that the expression in parentheses vanishes, which via matching translates into

$$-cv_{0n} + \partial_s v_{0t1} + \partial_u v_{0t2} = 0 \tag{57}$$

in the outer domain near the interface. Since the left-hand side is just the surface divergence on the interface, this is the desired incompressibility condition for the membrane. Formulas for a two-dimensional system can be easily obtained as a special case from the equations given here by setting $\tau=0$ and dropping all terms referring to the tangential direction $\mathbf{t}_2$.

IV. NUMERICAL STUDY OF THE PHASE-FIELD MODEL

The main numerical scheme is presented in Appendix C. Here we shall mainly present some of the numerical results. We first begin with the equilibrium shapes. It is now well established [18] that vesicles exhibit a variety of shapes. Of course we shall not intend to reproduce the whole list but simply give some typical results obtained by the PF model. We consider only the situation where the spontaneous curvature is set to zero. We are then left with the reduced volume only which is defined as

$$\tau = \frac{V}{(4\pi/3)(A/4\pi)^{3/2}}. \tag{58}$$

By definition $\tau=1$ for a sphere and $\tau<1$ otherwise. The strategy is the following. We start with an arbitrary shape characterized by a given τ. Then the vesicle shape evolves in time. The motion is limited by the hydrodynamic flow inside and outside the vesicle. After a certain time the vesicle attains its final equilibrium shape. Figure 1 shows series of equilibrium shapes for various τ. At large τ the shape is spherical with a transition towards a prolate shape at about $\tau=0.8$. The prolate shape enjoys an axial symmetry about the vertical axis in the figure. Another typical shape is the oblate one reproduced in Fig. 2. The oblate shape coexists [18] with the prolate one in a certain range of swelling factor; that is to say the prolate or oblate transition is of first order. Several other shapes could be obtained but we shall limit ourselves to these typical examples.

The next questions treated here is tanktreading and tumbling. In 2D we have recently extensively discussed the tumbling transition [13,21]. In 3D we expect additional richness not present in 2D due to the higher degree of deformability in 3D. The full discussion of this topic will constitute the subject of a future publication. Here we focus on testability of the PF model rather than on a systematic study of the dynamical transition themselves. Figure 3 shows a vesicle with no viscosity contrast and oriented in a linear shear flow which is similar to the problem studied in [5].

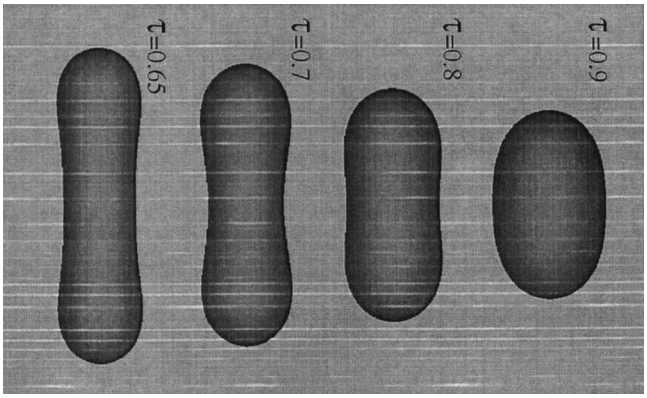

FIG. 1. The final stage of the evolution showing thus the equilibrium shapes for various values of the swelling factor in the prolate regime.

V. DISCUSSION

The first objective of the present paper was to extend the PF model for vesicles introduced in Ref. [13] to 3D. The second objective was to show formally that the PF equations reduce, to leading order, to the sharp boundary ones in the limit where $\epsilon \to 0$. The third objective was to show some sample results of evolution towards equilibrium shapes, and also some out of equilibrium results (tanktreading under shear flow). The virtue of the PF model lies in its flexibility to implement various effects without additional complication, and its natural ability of handling topology changes. In addition no explicit boundary tracking is required. Let us cite one example of flexibility used here. In the usual boundary integral formulation [6] even the introduction of a viscosity contrast requires some great deal, like adding [21] new integral terms related to the so-called *double layer* contribution, handling new singularities, etc. With the PF model this task requires just a change of the numbers η_{in} and η_{out} in the definition of the viscosity $\eta=(1-\phi)\eta_{in}/2+(1+\phi)\eta_{out}/2$. Another important virtue of the PF model in comparison to boundary integral formulation is the fact that the PF model

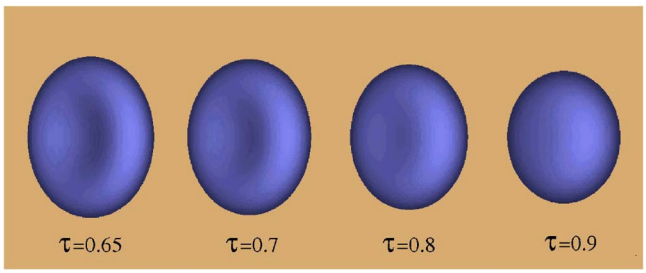

FIG. 2. (Color online) The final stage of the evolution showing thus the equilibrium shapes for various values of the swelling factor in the oblate regime.

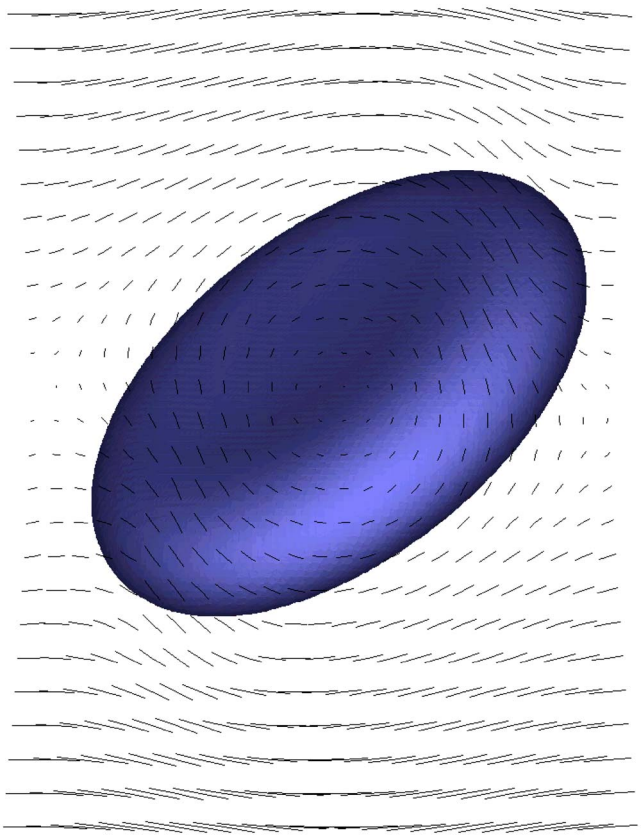

FIG. 3. (Color online) A vesicle under shear flow executing a tanktreading and oriented with an angle (less that $\pi/4$) in the flow.

can handle nonlinear constitutive laws, like for example non-Newtonian fluids.

Of course in order to obtain fully quantitative results with the PF model ϵ, the transition width must be small enough and usually one needs to extrapolate the results to $\epsilon=0$, as demonstrated for the tumbling transition in Ref. [22]. This task is of course time consuming and there is presently a need for a numerical speeding up. One possible way would be to make use of the so-called *thin boundary limit*. This task was performed in the solidification problem [23], a situation which has proven to lend itself to a remodeling of the problem in a way that allows an efficient suppression of spurious-slike terms introduced by the PF model, and therefore allowed to obtain quantitative results even with ϵ not too small. Whether this is possible or not within the PF model of vesicles is a question under investigation. Secondly, it will be also worthwhile to implement other schemes such as a multigrid or an adaptative scheme which have proven to be efficient in some PF models [24]. These two lines of research are now essential if one wants to take full advantage of the PF model.

Finally let us quote some questions which have not been incorporated in the model. We have not considered yet the case where the two monolayers may slide with respect to each other, instead of forming the same entity. This sliding results in an additional dissipation which may become essential for small enough vesicles [25]. In order to incorporate this effect one way would be to add to the Stokes equation a term like $\lambda\hat{\mathbf{n}}\cdot\boldsymbol{\nabla}\mathbf{v}$ where λ is a dissipation coefficient. We have not considered the case where a fluid exchange between the interior and exterior may occur. This effect can be retained by supposing that the phase field is not advected by the true fluid velocity, but by the fluid velocity from which we subtract $\mu\Delta p$, where Δp is a pressure difference between inside and outside, and μ is a permeability coefficient. We hope to deal with these two effects in the near future. Finally, in order to deal with more complex entities, like cells, we need to incorporate the elasticity (or even viscoelasticity) of the cytoskeleton. These questions constitute wide and interesting lines of future inquiries which embraces various communities going from physics to biology.

ACKNOWLEDGMENTS

This work is supported by the CNES (Centre National d'Etudes Spatiales) and by a French-Germain cooperation programme PROCOPE Grant No. D/0122928 and 04643YK. Financial support from a CNRS ACI grant from the "Mathematiques de la Cellule et du Myocarde" is acknowledged.

APPENDIX A: DERIVATION OF THE MEMBRANE FORCES

1. The curvature force

If c_1 and c_2 denote the two principal curvatures at a point of the surface, the curvature Hamiltonian can be written, after [20]

$$H_c = \frac{\kappa}{2}\int (c_1 + c_2 - c_0)^2 dA, \tag{A1}$$

where c_s accounts for a possible spontaneous curvature of the membrane. With the notations

$$\hat{c} = c_1 + c_2, \tag{A2}$$

the Hamiltonian (A1) can be rewritten:

$$H_c = \frac{\kappa}{2}\int (\hat{c} - c_0)^2 dA. \tag{A3}$$

The PF expression for the Hamiltonian can be obtained by inserting the shape function of the interface and extending the integral to the whole space:

$$H_C = \frac{\kappa}{2}\int (\hat{c} - c_0)^2 \delta_{shape}(\mathbf{r}) d\mathbf{r}, \tag{A4}$$

where $\hat{c}$ is now a curvature field defined at any point $\mathbf{r}$ of the 3D space (the "hat" on the variable is to remind us of this fact). The curvature field can be easily defined from the AF through the normal vector field $\hat{\mathbf{n}}$:

$$\hat{\mathbf{n}} = \frac{\boldsymbol{\nabla}\phi}{|\boldsymbol{\nabla}\phi|},$$

$$\hat{c} = -\boldsymbol{\nabla}\cdot\hat{\mathbf{n}}. \tag{A5}$$

Note that this prescription corresponds to a negative curvature for a sphere, and thanks to its definition (A2) a unit

sphere corresponds to $\hat{c}=-2$. The shape function $\delta_{shape}(\mathbf{r})$ can be chosen as

$$\delta_{shape}(\mathbf{r}) = \frac{|\nabla\phi(\mathbf{r})|}{2} \tag{A6}$$

which satisfies the normalization condition since the PF varies between −1 and +1.

The curvature force can be derived from the Hamiltonian by considering an elementary local displacement $\delta\mathbf{R}$ of the interface. In such a case the AF becomes $\phi(\mathbf{r}) \rightarrow \phi(\mathbf{r}-\delta\mathbf{R})$ so that

$$\delta\phi = -\nabla\phi \cdot \delta\mathbf{R} \tag{A7}$$

and the corresponding variations of $\hat{\mathbf{n}}$, c and δ_{shape} write

$$\delta\hat{\mathbf{n}} = (1-\hat{\mathbf{n}}\hat{\mathbf{n}}) \cdot \frac{\nabla\delta\phi}{|\nabla\phi|},$$

$$\delta\hat{c} = -\nabla \cdot \delta\hat{\mathbf{n}},$$

$$\delta(\delta_{shape}(\mathbf{r})) = \frac{\hat{\mathbf{n}} \cdot \nabla\delta\phi}{2}. \tag{A8}$$

The variation of the Hamiltonian can be obtained from its expression (A4):

$$\delta H_c = \frac{\kappa}{2}\int \{2(\hat{c}-c_0)\delta\hat{c}\,\delta_{shape} + (\hat{c}-c_0)^2\delta[\delta_{shape}(\mathbf{r})]\}d\mathbf{r}. \tag{A9}$$

Inserting (A8) into (A9) leads to

$$\delta H_c = \frac{\kappa}{2}\int \left\{-2(\hat{c}-c_0)\frac{|\nabla\phi|}{2}\nabla \cdot \left[(1-\hat{\mathbf{n}}\hat{\mathbf{n}}) \cdot \frac{\nabla\delta\phi}{|\nabla\phi|}\right] + (\hat{c}-c_0)^2\frac{\hat{\mathbf{n}} \cdot \nabla\delta\phi}{2}\right\}d\mathbf{r} \tag{A10}$$

a first integration by parts, assuming the cancellation of the fields at infinity, or periodic boundary conditions, yields

$$\delta H_c = \frac{\kappa}{2}\int \left\{2\nabla\left((\hat{c}-c_0)\frac{|\nabla\phi|}{2}\right) \cdot \left[(1-\hat{\mathbf{n}}\hat{\mathbf{n}}) \cdot \frac{\nabla\delta\phi}{|\nabla\phi|}\right] - \nabla \cdot \left(\frac{(\hat{c}-c_0)^2\hat{\mathbf{n}}}{2}\right)\delta\phi\right\}d\mathbf{r}, \tag{A11}$$

a second integration by parts allows us to put $\delta\phi$ as a common prefactor

$$\delta H_c = \frac{\kappa}{2}\int \nabla \cdot \left\{-2\frac{(1-\hat{\mathbf{n}}\hat{\mathbf{n}})}{|\nabla\phi|} \cdot \nabla\left((\hat{c}-c_0)\frac{|\nabla\phi|}{2}\right) - \frac{(\hat{c}-c_0)^2\hat{\mathbf{n}}}{2}\right\}\delta\phi d\mathbf{r}, \tag{A12}$$

and we can deduce from this expression, using Eq. (A7),

$$\mathbf{F}_c \equiv -\frac{\delta H_c}{\delta\mathbf{R}} = -\frac{\kappa}{2}\left\{\nabla \cdot \left[\frac{(1-\hat{\mathbf{n}}\hat{\mathbf{n}})}{|\nabla\phi|} \cdot \nabla[(\hat{c}-c_0)|\nabla\phi|]\right] + \nabla \cdot \left(\frac{(\hat{c}-c_0)^2}{2}\hat{\mathbf{n}}\right)\right\}\nabla\phi. \tag{A13}$$

2. The tension force

This force results from the constraint of fixed local area. This constraint is usually accounted for by introducing in the Hamiltonian a local Lagrange parameter field $\zeta(\mathbf{r})$ as

$$H_\zeta = T\int \zeta(\mathbf{r})dA.$$

The generalization of this expression to the AF framework is simply

$$H_\zeta = T\int \zeta(\mathbf{r})\delta_{shape}(\mathbf{r})d\mathbf{r}. \tag{A14}$$

An elementary displacement of the interface by $\delta\mathbf{R}$ leads, as previously, to

$$\delta\xi = -\nabla\xi \cdot \delta\mathbf{R},$$

$$\delta[\delta_{shape}] = \frac{\hat{\mathbf{n}} \cdot \nabla\delta\phi}{2}.$$

The variation of H_ξ writes

$$\delta H_\xi = T\int \left(\xi\frac{\hat{\mathbf{n}} \cdot \nabla\delta\phi}{2} - \delta\mathbf{R} \cdot \nabla\xi\delta_{shape}\right)d\mathbf{r}.$$

Integration by part of the first term yields

$$\delta H_\xi = T\int -\nabla \cdot \left(\xi\frac{\hat{\mathbf{n}}}{2}\right)\delta\phi - \delta\mathbf{R} \cdot \nabla\xi\delta_{shape}d\mathbf{r}.$$

Using $\delta\phi = -\nabla\phi \cdot \delta\mathbf{R}$, we easily identify the functional derivative of H_ξ:

$$\frac{\delta H_\xi}{\delta\mathbf{R}} = T[\nabla \cdot (\xi\hat{\mathbf{n}})\delta_{shape}\hat{\mathbf{n}} - \nabla\xi\delta_{shape}].$$

The tension force thus writes

$$\mathbf{F}_\xi \equiv -\frac{\delta H_\xi}{\delta\mathbf{R}} = T[-\nabla \cdot (\xi\hat{\mathbf{n}})\hat{\mathbf{n}} + \nabla\xi]\delta_{shape}$$

expanding $\nabla \cdot (\xi\hat{\mathbf{n}}) = \hat{\mathbf{n}} \cdot \nabla\xi + \xi\nabla \cdot \hat{\mathbf{n}} = \hat{\mathbf{n}} \cdot \nabla\xi - \xi\hat{c}$, the tension force can be expressed as

$$\mathbf{F}_\xi = T[(1-\hat{\mathbf{n}}\hat{\mathbf{n}}) \cdot \nabla\xi + \hat{c}\xi\hat{\mathbf{n}}]\delta_{shape}. \tag{A15}$$

APPENDIX B: EXPRESSION OF VARIOUS QUANTITIES USED IN THE SHARP BOUNDARY LIMIT

As seen in the main part of the paper, the metric reads

$$(g_{ij}) = \mathbf{g} = \begin{pmatrix} 1 & 0 & 0 \\ 0 & (1-rc_1)^2 + r^2\tau^2 & -2r\tau + r^2(c_1+c_2)\tau \\ 0 & -2r\tau + r^2(c_1+c_2)\tau & (1-rc_2)^2 + r^2\tau^2 \end{pmatrix}, \tag{B1}$$

its determinant is

$$g \equiv \det \mathbf{g} = [(1-rc_1)(1-rc_2) - r^2\tau^2]^2, \tag{B2}$$

and the contravariant version of the metric tensor takes the form

$$(g^{ij}) = \mathbf{g}^{-1} = \frac{1}{g}\begin{pmatrix} g & 0 & 0 \\ 0 & (1-rc_2)^2 + r^2\tau^2 & 2r\tau - r^2(c_1+c_2)\tau \\ 0 & 2r\tau - r^2(c_1+c_2)\tau & (1-rc_1)^2 + r^2\tau^2 \end{pmatrix}. \tag{B3}$$

The vectors of the reciprocal basis are given by $\mathcal{E}^i = g^{ij}\mathcal{E}_j$ (we use the Einstein summation convention throughout):

$$\mathcal{E}^r = \nabla r = \mathbf{n}(s,u),$$

$$\mathcal{E}^s = \nabla s = \frac{1}{\sqrt{g}}[(1-rc_2)\mathbf{t}_1 + r\tau\mathbf{t}_2],$$

$$\mathcal{E}^u = \nabla u = \frac{1}{\sqrt{g}}[(1-rc_1)\mathbf{t}_2 + r\tau\mathbf{t}_1]. \tag{B4}$$

We are now in a position to express differential operators in terms of the inner coordinates. The gradient is given by

$$\begin{aligned}\nabla &= \mathcal{E}^i\partial_i \\ &= \mathbf{n}\partial_r + \frac{1}{(1-rc_1)(1-rc_2) - r^2\tau^2}\{\mathbf{t}_1[(1-rc_2)\partial_s + r\tau\partial_u] \\ &\quad + \mathbf{t}_2[r\tau\partial_s + (1-rc_1)\partial_u]\},\end{aligned} \tag{B5}$$

and the divergence by

$$\begin{aligned}\nabla\cdot\mathbf{A} &= \frac{1}{\sqrt{g}}\partial_i(\sqrt{g}g^{ij}A_j) \\ &= \partial_r A_n - \frac{c_1+c_2-2r(c_1c_2-\tau^2)}{(1-rc_1)(1-rc_2)-r^2\tau^2}A_n \\ &\quad + \frac{1}{(1-rc_1)(1-rc_2)-r^2\tau^2}\{(1-rc_2)\partial_s A_{t1} \\ &\quad + (1-rc_1)\partial_u A_{t2} + r\tau(\partial_s A_{t2} + \partial_u A_{t1})\},\end{aligned} \tag{B6}$$

where $\mathbf{A}$ is some arbitrary vector, and terms containing derivatives of the curvatures and torsions cancel each other due to Eqs. (17). The general formula for the Laplacian is

$$\nabla^2 = \frac{1}{\sqrt{g}}\partial_i\sqrt{g}g^{ij}\partial_j, \tag{B7}$$

but we will not write out this expression explicitly, as it is very lengthy and all we need are the first few terms of its expansion in powers of ϵ.

Applying the formula for the divergence to the vector $\mathbf{A} = \mathbf{n}$ at $r=0$, we find immediately that the mean curvature of the interface is given by

$$c \equiv -\nabla\cdot\mathbf{n} = c_1 + c_2, \tag{B8}$$

i.e., it is the sum of *any* two normal curvatures corresponding to orthogonal directions, not just the sum of the two principal curvatures. Moreover, we can evaluate (9) on the interface $r=0$, which provides us with the Gaussian curvature there

$$G = \det[(\mathbf{t}_1\cdot\nabla)\mathbf{n}, (\mathbf{t}_2\cdot\nabla)\mathbf{n}, \mathbf{n}] = \mathbf{n}(\partial_s\mathbf{n}\times\partial_u\mathbf{n}) = c_1c_2 - \tau^2, \tag{B9}$$

from which we may conclude that if our geodesics happen to have the directions corresponding to the principal curvatures, the torsion will vanish.

The next step is to perform a stretching transformation via introduction of a fast coordinate $\rho = r/\epsilon$. The resulting expressions for differential operators are trivially obtained from Eqs. (B5)–(B7): each derivative with respect to r acquires a factor $1/\epsilon$ when replaced by a derivative with respect to ρ. Expanding the operators in powers of ϵ to the three leading orders, we obtain

$$\begin{aligned}\nabla &= \frac{1}{\epsilon}\mathbf{n}\partial_\rho \\ &\quad + \mathbf{t}_1\left\{\frac{1}{1-\epsilon\rho c_1}\partial_s + \epsilon\rho\tau\partial_u\right\} + \mathbf{t}_2\left\{\frac{1}{1-\epsilon\rho c_2}\partial_u + \epsilon\rho\tau\partial_s\right\} \\ &\quad + O(\epsilon^2),\end{aligned} \tag{B10}$$

$$\begin{aligned}\nabla\cdot\mathbf{A} &= \frac{1}{\epsilon}\partial_\rho A_n - \left(\frac{c_1}{1-\epsilon\rho c_1} + \frac{c_2}{1-\epsilon\rho c_2} + 2\epsilon\rho\tau^2\right)A_n \\ &\quad + \frac{1}{1-\epsilon\rho c_1}\partial_s A_{t1} + \frac{1}{1-\epsilon\rho c_2}\partial_u A_{t2} \\ &\quad + \epsilon\rho\tau(\partial_s A_{t2} + \partial_u A_{t1}) + O(\epsilon^2),\end{aligned} \tag{B11}$$

$$\begin{aligned}\nabla^2 &= \frac{1}{\epsilon^2}\partial_\rho^2 - \left(\frac{c_1}{1-\epsilon\rho c_1} + \frac{c_2}{1-\epsilon\rho c_2} + 2\epsilon\rho\tau^2\right)\frac{1}{\epsilon}\partial_\rho + \partial_s^2 + \partial_u^2 \\ &\quad + O(\epsilon).\end{aligned} \tag{B12}$$

With the three leading orders written out explicitly, the sought-for equations then read

$$\begin{aligned}&\partial_t\Phi - \frac{1}{\epsilon}W_n\partial_\rho\Phi - W_{t1}\partial_s\Phi - W_{t2}\partial_s\Phi \\ &\quad = -\frac{1}{\epsilon}V_n\partial_\rho\Phi - V_{t1}\partial_s\Phi - V_{t2}\partial_u\Phi \\ &\quad\quad + \Gamma\left(\frac{1}{\epsilon^2}\partial_\rho^2\Phi - (c+\epsilon\rho c^2 - 2\epsilon G)\frac{1}{\epsilon}\partial_\rho\Phi + \partial_s^2\Phi + \partial_u^2\Phi\right. \\ &\quad\quad \left. - \frac{1}{4\epsilon^2}g'(\Phi) + (c+\epsilon\rho c^2 - 2\epsilon G)\frac{1}{\epsilon}\partial_\rho\Phi\right) + O(\epsilon),\end{aligned} \tag{B13}$$

$$\epsilon_v\left(\partial_t\mathbf{V}-\frac{1}{\epsilon}W_n\partial_\rho\mathbf{V}-W_{t1}\partial_s\mathbf{V}-W_{t2}\partial_u\mathbf{V}\right)$$
$$=\eta\left(\frac{1}{\epsilon^2}\partial_\rho^2\mathbf{V}-(c+\epsilon\rho c^2-2\epsilon G)\frac{1}{\epsilon}\partial_\rho\mathbf{V}+\partial_s^2\mathbf{V}+\partial_u^2\mathbf{V}\right)$$
$$-\mathbf{n}\frac{1}{\epsilon}\partial_\rho P-\mathbf{t}_1\partial_s P-\mathbf{t}_1\partial_s P+\mathbf{F}_c+\mathbf{F}_\xi+O(\epsilon), \quad \text{(B14)}$$

$$\mathbf{F}_c=-\kappa\left\{\frac{1}{2}c(c^2-4G)+(\partial_s^2+\partial_u^2)c+O(\epsilon)\right\}\frac{1}{2\epsilon}\partial_\rho\Phi, \quad \text{(B15)}$$

$$\mathbf{F}_\xi=\frac{\tilde{T}}{\epsilon}\{Xc\mathbf{n}+(\mathbf{t}_1\partial_s+\mathbf{t}_2\partial_u)X+O(\epsilon)\}\frac{1}{2\epsilon}\partial_\rho\Phi, \quad \text{(B16)}$$

$$\frac{1}{\epsilon}\partial_\rho V_n-(c+\epsilon\rho c^2-2\epsilon G)V_n+\partial_s V_{t1}+\partial_u V_{t2}=O(\epsilon^2), \quad \text{(B17)}$$

$$\partial_t X-\frac{1}{\epsilon}W_n\partial_\rho X-W_{t1}\partial_s X-W_{t2}\partial_u X$$
$$=+D_\xi\left(\frac{1}{\epsilon^2}\partial_\rho^2 X-(c+\epsilon\rho c^2-2\epsilon G)\frac{1}{\epsilon}\partial_\rho X+\partial_s^2 X+\partial_u^2 X\right)$$
$$-\frac{1}{\epsilon}V_n\partial_\rho X-V_{t1}\partial_s X-V_{t1}\partial_u X-cV_n+\partial_s V_{t1}+\partial_u V_{t2}$$
$$+O(\epsilon). \quad \text{(B18)}$$

Note that in (B13), the second and last terms in the parentheses multiplied by Γ cancel each other, by construction. The forces described by Eqs. (B15) and (B16) are only given to $O(1)$, since this is the second subdominant order of Eq. (B14). These equations are used in the main part of the paper in order to derive the inner equations.

APPENDIX C: NUMERICAL SCHEMES

The fluid is considered as being incompressible, so that

$$\nabla\cdot\mathbf{v}=0. \quad \text{(C1)}$$

The Stokes equation is solved in practice using a relaxation scheme:

$$\epsilon_v\frac{\partial\mathbf{v}}{\partial t}=\nabla\cdot[\eta(\phi)\{\nabla\mathbf{v}+(\nabla\mathbf{v})^T\}]-\nabla P+\mathbf{F}, \quad \text{(C2)}$$

where ϵ_v controls the relaxation time scale. ϵ_v is a density that can be used to build a Reynolds number (of the order of 10^{-2} in practice). Equation (C2) can be rewritten:

$$\epsilon_v\frac{\partial\mathbf{v}}{\partial t}=\eta(\phi)\Delta\mathbf{v}+\eta'(\phi)\nabla\phi\cdot\{\nabla\mathbf{v}+(\nabla\mathbf{v})^T\}-\nabla P+\mathbf{F}, \quad \text{(C3)}$$

where we have explicitly used the incompressibility condition (C1), and $\eta'(\phi)\equiv d\eta/d\phi$. $\mathbf{F}$ is the full force acting on the membrane (bending and tensionlike force).

Due to the $\Delta\mathbf{v}$ term, a direct Euler integration scheme is subjected to numerical instabilities when the time step is too large. Two possibilities exist to cope with this problem: reducing the time step or using an implicit scheme. The second solution is very powerful since it suppresses the instability due to the Laplacian contribution. We can however not use this scheme in a strict way due to the nonlinearity introduced by the spatial variation of the viscosity field $\eta(\phi)$, rather, we can implement a mixed scheme by subtracting $\eta_{max}\Delta\mathbf{v}$ from both sides of Eq. (C3), where η_{max} is the largest value of the viscosity in the system. Equation (C3) is therefore rewritten as

$$\left[\epsilon_v\frac{\partial}{\partial t}-\eta_{max}\Delta\right]\mathbf{v}=[\eta(\phi)-\eta_{max}]\Delta\mathbf{v}-\nabla P+\mathbf{F}$$
$$+\eta'(\phi)\nabla\phi\cdot\{\nabla\mathbf{v}+(\nabla\mathbf{v})^T\}. \quad \text{(C4)}$$

Although we use in practice a fourth order Runge-Kutta method for the temporal integration, it is interesting to consider a single implicit Euler integration step to emphasize the interest of Eq. (C4). The temporal derivation can be discretized as $\partial\mathbf{v}/\partial t\sim(\mathbf{v}^{t+dt}-\mathbf{v}^t)/dt$, where dt is the time step, and thus Eq. (C4) takes the discrete form:

$$\epsilon_v\frac{\mathbf{v}^{t+dt}-\mathbf{v}^t}{dt}-\eta_{max}\Delta\mathbf{v}^{t+dt}=[\eta(\phi^t)-\eta_{max}]\Delta\mathbf{v}^t-\nabla P+\mathbf{F}^t$$
$$+\eta'(\phi^t)\nabla\phi^t\cdot[\nabla\mathbf{v}^t+(\nabla\mathbf{v}^t)^T]. \quad \text{(C5)}$$

The implicit method consists in evaluating the Laplacian term on the left side at time $t+dt$. The velocity field at time $t+dt$ is then obtained by inverting:

$$\left(1-\eta_{max}\frac{dt}{\epsilon_v}\Delta\right)\mathbf{v}^{t+dt}=\mathbf{v}^t+\frac{dt}{\epsilon_v}\{[\eta(\phi)-\eta_{max}]\Delta\mathbf{v}-\nabla P+\mathbf{F}$$
$$+\eta'(\phi)\nabla\phi\cdot[\nabla\mathbf{v}+(\nabla\mathbf{v})^T]\}^t. \quad \text{(C6)}$$

This inversion can easily be done in the (spatial) Fourier space if periodic boundary conditions (PBC) apply at the edge of the resolution box. This is not indeed the case in general when the vesicle is placed in an external flow, like a simple shear for example, where a velocity difference is applied at two opposite sides of the resolution box. Interestingly, if the external applied flow is linear it does not contribute to the Laplacian term, it only contributes to the gradient tensor, and its contribution can be calculated analytically. Setting $\mathbf{v}=\mathbf{v}_{applied}+\mathbf{u}$, where the externally applied field $\mathbf{v}_{applied}$ is time independent and linear in space, and $\mathbf{u}$ is the velocity field induced by the vesicle, Eq. (C6) rewrites

$$\left(1-\eta_{max}\frac{dt}{\epsilon_v}\Delta\right)\mathbf{u}^{t+dt}=\mathbf{u}^t+\frac{dt}{\epsilon_v}\{[\eta(\phi)-\eta_{max}]\Delta\mathbf{u}-\nabla P+\mathbf{F}$$
$$+\eta'(\phi)\nabla\phi\cdot[\nabla\mathbf{v}+(\nabla\mathbf{v})^T]\}^t. \quad \text{(C7)}$$

Assuming PBC for the induced field $\mathbf{u}$ only, and noticing that the gradient tensor only plays a role in the vicinity of the interface thanks to the $\nabla\phi$ prefactor, this contribution cancels at the boundary of the resolution box and can then sat-

isfy PBC, this last equation can be inverted in Fourier space to give

$$\mathbf{u}_k^{t+dt} = \frac{1}{1+\eta_{max}\frac{dt}{\epsilon_v}k^2}\Bigg[\mathbf{u}_k^t + \frac{dt}{\epsilon_v}\{[\eta(\phi)-\eta_{max}]\Delta\mathbf{u} - \boldsymbol{\nabla}P + \mathbf{F} + \eta'(\phi)\,\boldsymbol{\nabla}\phi\cdot[\boldsymbol{\nabla}\mathbf{v}+(\boldsymbol{\nabla}\mathbf{v})^T]\}_k^t\Bigg], \tag{C8}$$

where index "k" denotes a spatial Fourier transformation of the quantity at wave vector k. The power of the implicit scheme comes from the property that $|1/(1+\eta_{max}(dt/\epsilon_v)k^2)| \leqslant 1$ for all wave vectors k whatever the value of dt, which ensures the stability of the iterative scheme in the absence of the term between braces (pure diffusion). Due to the presence of this extra term, the iterative scheme does not always converge, but instabilities occur at much larger values of dt. Interestingly, in the Fourier space the incompressibility condition (C1) simply states that the velocity field belongs to the transverse space. Pressure can then be eliminated by applying the projector on the transverse space:

$$\mathbf{u}_k^{t+dt} = \frac{1}{1+\eta_{max}\frac{dt}{\epsilon_v}k^2}\left(1-\frac{\mathbf{kk}}{k^2}:\right)\Bigg[\mathbf{u}_k^t + \frac{dt}{\epsilon_v}\{[\eta(\phi)-\eta_{max}]\Delta\mathbf{u} + \mathbf{F} + \eta'(\phi)\,\boldsymbol{\nabla}\phi\cdot[\boldsymbol{\nabla}\mathbf{v}+(\boldsymbol{\nabla}\mathbf{v})^T]\}_k^t\Bigg]. \tag{C9}$$

This equation allows for the computation of $\mathbf{u}_k^{t+dt}$ which after a backward Fourier transformation and addition of the applied velocity field leads to the velocity field $\mathbf{v}^{t+dt}$.

1. The AF equation

The AF equation is

$$\frac{\partial\phi}{\partial t} = -\mathbf{v}\cdot\boldsymbol{\nabla}\phi + \epsilon_\phi\left(-\frac{\delta E_{intrinsic}}{\delta\phi} + \hat{c}\epsilon^2|\boldsymbol{\nabla}\phi|\right) \tag{C10}$$

with $E_{intrinsic}=\int\{(1-\phi^2)^2/4+\epsilon^2\boldsymbol{\nabla}\phi^2/2\}d\mathbf{r}$ the AF equation becomes

$$\frac{\partial\phi}{\partial t} = -\mathbf{v}\cdot\boldsymbol{\nabla}\phi + \epsilon_\phi\{\phi(1-\phi^2)+\epsilon^2(\Delta\phi+\hat{c}|\boldsymbol{\nabla}\phi|)\}$$

again, numerical difficulties due to the Laplacian term can be expected in principle at large time steps, but thanks to the prefactor $\epsilon_\phi\epsilon^2$ this contribution remains small enough so that a standard explicit Euler scheme is sufficient:

$$\phi^{t+dt} = \phi^t + dt[-\mathbf{v}\cdot\boldsymbol{\nabla}\phi + \epsilon_\phi\{\phi(1-\phi^2)+\epsilon^2(\Delta\phi+\hat{c}|\boldsymbol{\nabla}\phi|)\}]^t. \tag{C11}$$

As for the velocity field, this elementary step is included in a fourth order Runge-Kutta method.

a. The Lagrange's parameter field

This field evolves following the dynamical equation:

$$\frac{\partial\xi}{\partial t} = -\mathbf{v}\cdot\boldsymbol{\nabla}\xi + T\boldsymbol{\nabla}_\parallel\cdot\mathbf{v}, \tag{C12}$$

where

$$\boldsymbol{\nabla}_\parallel\cdot\mathbf{v} = (1-\hat{\mathbf{n}}\hat{\mathbf{n}}):\boldsymbol{\nabla}\mathbf{v}.$$

Using a basic Euler scheme is not sufficient here due to the instable nature of the advective contribution. In the previous case of the AF, this advection instability was cured by the diffusive contribution ($\Delta\phi$) absent in the present case. A simple solution is to add a small diffusive contribution to Eq. (C12), in the spirit of the Lax scheme, but the diffusion coefficient we use in practice is much smaller than in the Lax method so that the solution remains accurate (see below).

From Eq. (C12) ξ is the temporal integral of $\boldsymbol{\nabla}_\parallel\cdot\mathbf{v}$ which represents the local elongation rate along an isocontour of the AF. $\boldsymbol{\nabla}_\parallel\cdot\mathbf{v}$ is defined everywhere in space, and thus ξ. In the vicinity of the membrane $\boldsymbol{\nabla}_\parallel\cdot\mathbf{v}$ remains small since the role of ξ is precisely to cancel elongation of the membrane. Far away from the membrane on the contrary, this constraint does not apply and $\boldsymbol{\nabla}_\parallel\cdot\mathbf{v}$ reaches arbitrary values in the steady regime. As a consequence, ξ reaches a steady state in the vicinity of the membrane only, its growth far away from the interface simply illustrates that two initially neighboring points can be transported arbitrarily far away after a given time. It is then interesting to truncate the variations of ξ at some distance from the interface to prevent the numerical noise induced by the irrelevant growth of ξ in these region to propagate in the interfacial region. To this end, we introduce a "gate" function $f(r)$, where r is the distance to the $\phi=0$ isocontour, which truncates $\boldsymbol{\nabla}_\parallel\cdot\mathbf{v}$ at a certain distance (its precise shape will be given below). The dynamical equation thus becomes

$$\frac{\partial\xi}{\partial t} = -\mathbf{v}\cdot\boldsymbol{\nabla}\xi + T\boldsymbol{\nabla}_\parallel\cdot\mathbf{v}f(r) + \epsilon_\xi\Delta\xi$$

and can now be solved on the basis of the Euler scheme:

$$\xi^{t+dt} = \xi^t + dt\{-\mathbf{v}\cdot\boldsymbol{\nabla}\xi + T\boldsymbol{\nabla}_\parallel\cdot\mathbf{v}f(r) + \epsilon_\xi\Delta\xi\}^t. \tag{C13}$$

Again, this elementary step is combined to a fourth order Runge-Kutta method.

b. Geometrical and auxiliary quantities

We specify now how geometrical quantities like the tangential, the normal vector fields or the curvature field are computed. From the knowledge of the AF at time t, the normal vector field can be calculated as

$$\hat{\mathbf{n}}(r) = \frac{\boldsymbol{\nabla}\phi}{\max(|\boldsymbol{\nabla}\phi|,\epsilon_n)}, \tag{C14}$$

where ϵ_n is a cutoff that prevents the cancellation of the denominator far away from the interface. $\hat{\mathbf{n}}$ is then normalized in the neighborhood of the interface only. ϵ_n is homogeneous to the inverse of a length. The tangent vectors $\hat{\mathbf{t}}$ and $\hat{\mathbf{m}}$ are easily obtained from $\hat{\mathbf{n}}$ by orthogonalization:

$$\hat{\mathbf{t}} = \hat{\mathbf{n}}\times\hat{\mathbf{w}},$$

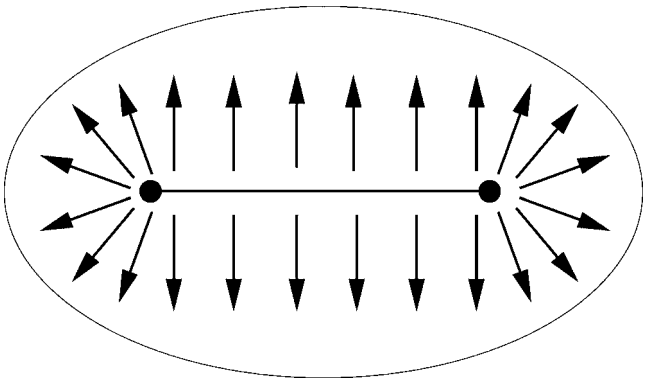

FIG. 4. Schematic drawing of the normal vector field inside the vesicle; the two points correspond to curvature centers and the line between then is a line singularity.

$$\hat{\mathbf{m}} = \hat{\mathbf{n}} \times \hat{\mathbf{t}}, \tag{C15}$$

where $\hat{\mathbf{w}}$ is an arbitrary normalized vector, the relevant physical quantities being independent of the precise choice of $\hat{\mathbf{w}}$. The Gaussian curvature "g" is computed through

$$g = (\hat{\mathbf{t}} \cdot \boldsymbol{\nabla}\hat{\mathbf{n}} \times \hat{\mathbf{m}} \cdot \boldsymbol{\nabla}\hat{\mathbf{n}}) \cdot \hat{\mathbf{n}}.$$

More difficult is the computation of the curvature field "$\hat{c}$." Expression $\hat{c} = -\boldsymbol{\nabla} \cdot \hat{\mathbf{n}}$ allows in principle for the computation of the curvature field everywhere $\hat{\mathbf{n}}(\mathbf{r})$ is regular, and is a unit vector. We then have to face two problems: singularities of $\hat{\mathbf{n}}(\mathbf{r})$, and the cutoff ϵ_n introduced in the normalization of $\hat{\mathbf{n}}$ to reduce the numerical noise. Cancellation of the norm of $\hat{\mathbf{n}}$ far away from the interface is not too problematic since all quantities related to the interface are weighted by $|\boldsymbol{\nabla}\phi|/2$, the shape function of the interface that cancels exponentially away from the interface. In the steady regime $\phi \sim \tanh(r/\epsilon\sqrt{2})$, where r is the coordinate in the normal direction, $r=0$ at the interface. We set $r^* = r/\epsilon\sqrt{2}$ in the following, $r^*=1$ corresponds to the typical range of the interface. The shape function is then $|\boldsymbol{\nabla}\phi|/2 = \{1-\tanh^2(r^*)\}/(2\sqrt{2}\epsilon)$. This function is maximum at $r^*=0$ and its value is $1/(2\sqrt{2}\epsilon)$. In practice, ϵ_n is chosen as $10^{-4}/(2\sqrt{2}\epsilon)$, implying that it plays a role in a region where the shape function is only 10^{-4} its maximum value. The results are then not affected much by this cutoff. The distance at which ϵ_n plays a role can be estimated as $r^*_{\epsilon_n} = 5.65$ which is relatively large compared to 1. The singularities of the normal vector field (as shown in Fig. 4) are more problematic since they can occur in the vicinity of the interface at finite values of ϵ. These singularities are of two types: point singularities, occurring at curvature centers, and line singularities which usually occur along symmetry axis. In principle these defects should not play any role in the dynamics of the interface in the sharp interface limit since they remain located at finite distances from the interface. However, at finite values of ϵ they can alter the results. These singularities can be removed in several ways. A first possibility is to regularize the normal vector field $\hat{\mathbf{n}}(\mathbf{r})$ before computing the divergence. A second possibility is to filter the resulting curvature field. We use both prescriptions in practice. The normal vector field can be regularized by forcing locally two adjacent normal vectors to have a positive scalar product during the computation of the divergence: if $\boldsymbol{\nabla}\cdot\hat{\mathbf{n}}$ is to be estimated at site "i," values of $\hat{\mathbf{n}}$ at adjacent sites will be chosen to be the actual value of $\hat{\mathbf{n}}$ if $\hat{\mathbf{n}}_i \cdot \hat{\mathbf{n}} > 0$ and $-\hat{\mathbf{n}}$ otherwise. This procedure is very efficient for line singularities, and smooth quite efficiently point singularities. To prevent the large values of the curvature field induced by point singularities to alter the interfacial region it is interesting to set the shape function to zero at some distance from the interface. This shape function is in practice rapidly decreasing but does not strictly cancel at finite distance. It is then interesting to use a "gate" function $f(r)$ (already mentioned above):

$$f(r) = \frac{1 - \tanh[10(|r^*| - r^*_{curv})]}{2}, \tag{C16}$$

where $r^* = r/(\sqrt{2}\epsilon)$ and $r^*_{curv} = 4$. $f(r)$ goes from 1, at distances lower than r^*_{curv}, to zero in a continuous, although quite rapid, way. Further, this function is truncated to exactly zero for $r^* > 5$. This function acts on the shape function through

$$\delta_{shape}(r) = \frac{\boldsymbol{\nabla}\phi}{2} f(r).$$

The truncation replaces values of δ_{shape} as small as 6.7×10^{-4} its maximum value by zero. From the values of $\phi(\mathbf{r})$, $\mathbf{v}(\mathbf{r})$ and $\xi(\mathbf{r})$ at time t, $\hat{\mathbf{n}}(\mathbf{r})$, $\hat{\mathbf{t}}(\mathbf{r})$, $\hat{\mathbf{m}}(\mathbf{r})$, $g(\mathbf{r})$ and $c(\mathbf{r})$ can be computed as explained above, and thus all the contributions appearing in the elementary equations (C9), (A4), and (C13) can be estimated to obtain the new values of $\phi(\mathbf{r})$, $\mathbf{v}(\mathbf{r})$ and $\xi(\mathbf{r})$ at time $t+dt$, provided we have a prescription for the differential operators.

c. Differential operators and boundary conditions

The precise prescription for the differential operators strongly depends on the mesh geometry. Since the velocity equation is simply solved in the Fourier space, it is interesting to use a cubic (or square in 2D) lattice with PBC. We have already discussed the particular case of the velocity field, for which PBC are applied to the induced component only (i.e., $\mathbf{v} - \mathbf{v}_{applied}$). PBC apply quite naturally to the AF $\phi(\mathbf{r})$ and $\xi(\mathbf{r})$, since these quantities vanish far away from the interface, and are thus close to zero at the edge of the resolution box. We have checked that for boxes as large as ten times the diameter of the vesicle, PBS do not alter the results in a significant way. Care must be taken for the discrete formulation of the differential operators since isotropy plays a key role here. We use in practice isotropic order h^2 operators, where h is the grid spacing. If $\delta g_{y,z} \equiv g(x+h,y,z) - g(x-h,y,z)$, a partial derivative along the x axis is computed as

$$\frac{\partial g}{\partial x} = \frac{1}{12h}[2\delta g_{y,z} + \delta g_{y+h,z} + \delta g_{y-h,z} + \delta g_{y,z+h} + \delta g_{y,z-h}],$$

where g is a generic function, This prescription ensures that the computed gradient is not sensitive to the orientation of the grid up to order h^4 (h^4 excluded). the first corrective term is of order h^2 and is isotropic. The same care must be taken

for second order derivatives, the isotropic Laplacian of order h^2 writes

$$\Delta = \frac{1}{6h^2}[\Sigma_1 + 2\Sigma_2 - 24g(x,y,z)],$$

where

$$\Sigma_1 = \sum [g(x,y \pm h,z \pm h) + g(x \pm h,y,z \pm h) + g(x \pm h,y \pm h,z)],$$

$$\Sigma_2 = \sum [g(x \pm h,y,z) + g(x,y \pm h,z) + g(x,y,z \pm h)].$$

d. Relevant and auxiliary parameters

The physical parameters are as follows.

κ is the curvature modulus.

c_0 is the spontaneous curvature.

T is the tension modulus of the membrane (which strictly speaking should be infinite for a vesicle).

η_{in}, η_{out} are the two viscosities.

R is the vesicle size (radius of the sphere of equal volume in 3D, area in 2D).

τ is the swelling ratio of the initial configuration.

γ is the shear rate. $1/\gamma$ is the time scale associated to the external flow.

ϵ_v is indeed a technical parameter here, but it defines a mass scale and therefore introduces some inertia in the problem.

These eight parameters can be combined to define the three time, mass and length scales, and five dimensionless control parameters.

To construct the dimensionless parameters, it is interesting to consider the various time scales entering in the problem.

$1/\gamma$ is the time scale forced by the imposed flow.

$\tau_\kappa = \eta_{out}R^3/\kappa$ is the typical relaxation scale of the curvature [26].

$\tau_T = \eta_{out}R/T$ is the typical relaxation time of the surface (3D)/ perimeter (2D) to its steady value.

We will choose τ_κ to define the unit time scale. This time corresponds to the natural relaxation time of the vesicle (τ_T should be ideally vanishingly small). Two dimensionless numbers can be constructed as

$$C_\kappa = \frac{\eta_{out}\gamma R^3}{\kappa},$$

$$C_T = \frac{\eta_{out}\gamma R}{T}.$$

These two parameters characterize the deformability of the vesicle in the imposed flow. C_κ controls the deformation of the global shape (competition between the curvature energy and the flow) whereas C_T controls the elongation of the membrane surface (perimeter). The larger these numbers, the larger the associated deformation.

Other time scales can be defined, inertial or viscous time scales, but we will introduce directly the dimensionless numbers associated with them.

$\mathrm{Re} = \epsilon_v \gamma R^2/\eta_{out}$ is the Reynolds number, or more generally the Suratman number $\mathrm{Su} = \mathrm{Re}/C_\kappa = \epsilon_v\kappa/\eta_{out}^2 R$ which is the Reynolds number based on τ_κ rather than $1/\gamma$. It has the advantage to be well defined even in the absence of external flow.

η_{in}/η_{out} is the viscosity ratio which defines the competition between the internal and external relaxation of the fluid.

The last dimensionless parameter is the swelling ratio τ, and the length and mass scales will be defined by R and ϵ_v.

2. Summary

Time length and mass scales are defined by

$$\tau_\kappa = \frac{\eta_{out}R^3}{\kappa} = 1,$$

$$R = 1,$$

$$\epsilon_v = 1.$$

The physical control parameters are

$$C_\kappa = \frac{\eta_{out}\gamma R^3}{\kappa} = \gamma\tau_\kappa, \text{ typical value: } 0.5,$$

$$C_T = \frac{\eta_{out}\gamma R}{T}, \text{ typical value: } 10^{-3},$$

weak extensibility of the membrane,

$$\mathrm{Su} = \mathrm{Re}/\mathrm{C} = \frac{\epsilon_v\kappa}{\eta_{out}^2 R}, \text{ typical value: } 10^{-2}, \text{ Stokes regime},$$

$p = \eta_{in}/\eta_{out}$, typically between 1 and 10,

τ, the swelling ratio, between 0.7 and 1,

$c_0 R$, the spontaneous curvature (zero in the present study).

We now discuss the technical parameters such as

ϵ, the width of the interface $\sim 0.035R$,

h, the grid spacing $\sim 0.03R$,

dt, the time step $\sim 10^{-3}\tau_\kappa$,

$\tau_\phi \equiv 1/\epsilon_\phi$, (fast) relaxation time of the AF $\sim 0.2\tau_\kappa$,

$\tau_\xi \equiv TR^2/\epsilon_\xi$, slow diffusion introduced for numerical stability purposes $\sim 400\tau_\kappa$,

$$\epsilon_n = 10^{-4}/(2\sqrt{2}\epsilon),$$

$$r_{curv} = 4\sqrt{2}\epsilon.$$

We finally need to specify the initial conditions. An initial guess for the velocity field $\mathbf{v}(\mathbf{r})$ [or equivalently $\mathbf{u}(\mathbf{r})$, the

flow induced by the vesicle], the AF $\phi(\mathbf{r})$ and the Lagrange's parameter field $\xi(\mathbf{r})$ (tension field) have to be chosen. The initial shape for the vesicle is chosen to be ellipsoidal since the swelling ratio can be at least numerically easily determined. The initial AF is then generated as $\phi(\mathbf{r}) = \tanh(r/\sqrt{2}\epsilon)$ where $r=0$ corresponds to the ellipsoid, and r is the coordinate in the direction of the outgoing normal vector. With the prescription $\phi<0$ inside the vesicle and $\phi>0$ outside, so that the gradient points outside the vesicle, and the normal vector field defined by (C14) also. The velocity field $\mathbf{u}(\mathbf{r})$ and the Lagrange's parameter field $\xi(\mathbf{r})$ are initially set to zero.

[1] Y. Saito, *Statistical Physics of Crystal Growth*, 1st ed. (World Scientific, Singapore, 1996).

[2] K. Kassner, *Pattern Formation in Diffusion-Limited Crystal Growth: Beyond the Single Dendrite* (World Scientific, Singapore, 1995).

[3] J. Eggers, Rev. Mod. Phys. **69**, 865 (1997).

[4] C. Pozrikidis, J. Fluid Mech. **440**, 269 (2001).

[5] M. Kraus, W. Wintz, U. Seifert, and R. Lipowsky, Phys. Rev. Lett. **77**, 3685 (1996).

[6] I. Cantat and C. Misbah, Phys. Rev. Lett. **83**, 235 (1999).

[7] K. Kassner and C. Misbah, Europhys. Lett. **28**, 245 (1994).

[8] C. H. Chui and H. Gao, Int. J. Solids Struct. **30**, 2983 (1993).

[9] G. Caginalp, Phys. Rev. A **39**, 5887 (1989), and references therein.

[10] K. Kassner and C. Misbah, Europhys. Lett. **46**, 217 (1999).

[11] J. Müller and M. Grant, Phys. Rev. Lett. **82**, 1736 (1999).

[12] A. Karma and A. E. Lobkovsky, Phys. Rev. Lett. **92**, 245510 (2004).

[13] T. Biben and C. Misbah, Eur. Phys. J. B **29**, 311 (2002); T. Biben and C. Misbah, Phys. Rev. E **67**, 031908 (2003); T. Biben, C. Misbah, A. Leyrat, and C. Verdier, Europhys. Lett. **63**, 623 (2003).

[14] Q. Du, C. Liu, and X. Wang, J. Comput. Phys. **198**, 450 (2004).

[15] R. Folch, J. Casademunt, A. Hernández-Machado, and L. Ramirez-Piscina, Phys. Rev. E **60**, 1724 (1999).

[16] D. Gueyffier *et al.*, J. Comput. Phys. **152**, 423 (1999).

[17] M. Sussman, P. Smereka, and S. Osher, J. Comput. Phys. **114**, 146 (1994).

[18] *Structure and Dynamics of Membranes*, Handbook of Biological Physics, edited by R. Lipowsky and E. Sackmann (Elsevier, North-Holland, Amsterdam, 1995).

[19] *Mathematik-Handbuch für Technik und Naturwissenschaft*, edited by J. Dreszer (Verlag Harri Deutsch, Züfcrich, 1975), p. 518.

[20] O.-Y. Zhong-can and W. Helfrich, Phys. Rev. A **39**, 5280 (1989).

[21] F. Rioual, T. Biben, and C. Misbah, Phys. Rev. E **69**, 061914 (2004).

[22] J. Beaucourt, F. Rioual, T. Séon, T. Biben, and C. Misbah, Phys. Rev. E **69**, 011906 (2004).

[23] A. Karma and W. J. Rappel, Phys. Rev. E **57**, 4323 (1998).

[24] Y. W. Zhang and A. F. Bower, J. Mech. Phys. Solids **47**, 2273 (1999).

[25] U. Seifert and S. A. Langer, Europhys. Lett. **23**, 71 (1993).

[26] In principle we should use the largest viscosity (η_{in} or η_{out}) to estimate this time scale. In practice the viscosity ratio will vary between 1 and 10, which remains of the order of the geometrical prefactors we have not included in these definitions. Moreover, the viscosity of the external fluid is experimentally much easier to control than the viscosity of the encapsulated fluid. This motivated our choice.